KINEMATICS AND DYNAMICS ANALYSIS FOR A HOLONOMIC WHEELED MOBILE ROBOT

Ahmed El-Shenawy, Achim Wagner and Essam Badreddin
Computer Engineering, University of Mannheim , B6. 23-27 part B, Mannheim, Germany

Keywords: Modeling, Robot Kinematics, Robot Dynamics, Analysis.

Abstract: This paper presents the kinematics and the dynamics analysis of the holonomic mobile robot C3P. The robot has three caster wheels with modular wheel angular velocities actuation. The forward dynamics model which is used during the simulation process is discussed along with the robot inverse dynamics solution. The inverse dynamics solution is used to overcome the singularity problem, which is observed from the kinematic modeling. Since both models are different in principle they are analyzed using simulation examples to show the effect of the actuated and non actuated wheel velocities on the robot response. An experiment is used to illustrate the performance of the inverse dynamic solution practically.

1 INTRODUCTION

Wheeled mobile robots became an important tool in our daily life. They are found in a multitude of application such as guiding disabled people in museums (Burgard et al., 2002; Steinbauer and Wotawa, 2004) and hospitals (Kartoun et al., 2006), transporting goods in warehouses, manipulation of army explosives (Bruemmer et al., 1998), or securing important facilities (Chakravarty et al., 2004).

Wheeled mobile robots are categorized into two main types: *holonomic* and *non-holonomic*, which are the mobility constraints of the mobile robot platform (Yun and Sarkar, 1998). A holonomic configuration implies that the number of robot velocities DOF (**D**egrees **O**f **F**reedom) is equal to the number of position coordinates. The main advantage of holonomic mobility is the ability of efficient maneuvering in narrow places. In the last two decades, many considerable research efforts addressing the mobility of holonomic wheeled mobile robots were done (Fulmer, 2003; Moore and Flann, 2000) and (Yamashita et al., 2001).

Usually, kinematic modeling is used in the field of WMRs (**W**heeled **M**obile **R**obot) to obtain stable motion control laws for trajectory following or goal reaching (Khatib et al., 1997; Ramírez and Zeghloul, 2000). Using the dynamics modeling during the simulation process results in a better control design. By comparing its results to the practical implementation, a better precision and more variables assumption are achieved in comparison to the kinematics model.

The dynamic modeling is much more complex than the kinematic modeling. Furthermore, the kinematic modeling is required for deriving the dynamic model. Hence, it is assumed that the velocity and acceleration solutions can be solved without any difficulty. Generally, the main property of the dynamic model is that it involves the forces that act on the multibody system and its inertial parameters such as : mass, inertia, with respect to the center of gravity (Albagul and Wahyudi, 2004; Asensio and Montano, 2002).

The holonomic mobile robot "C3P" (**C**aster **3** wheeled **P**latform) is described geometrically in section 2. The singularity problem found in the C3P configuration is illustrated in section 3 through the kinematic analysis. The forward dynamic model and the inverse dynamic solution are presented and analyzed in section 4 to show their different structure. Few simulation examples are shown to illustrate the effect of the actuated and non-actuated variables on the robot behavior using the inverse dynamic solution. In section 5, a lab experiment is presented to show the per-

El-Shenawy A., Wagner A. and Badreddin E. (2007).
KINEMATICS AND DYNAMICS ANALYSIS FOR A HOLONOMIC WHEELED MOBILE ROBOT.
In *Proceedings of the Fourth International Conference on Informatics in Control, Automation and Robotics*, pages 485-491
DOI: 10.5220/0001650404850491

formance of the solution on the practical implemented module.

2 THE PLATFORM CONFIGURATION

The C3P WMR is a holonomic mobile robot, which is previously discussed in (Peng and Badreddin, 2000). The C3P has three caster wheels attached to a triangular shaped platform with smooth rounded edges as shown in Fig. (1). Each caster wheel is attached to each hip of the platform. The platform origin coordinates are located at its geometric center, and the wheels are located with distance h from the origin and $\alpha_1 = 30^o$, $\alpha_2 = 150^o$, and $\alpha_3 = 270^o$ shifting angles,

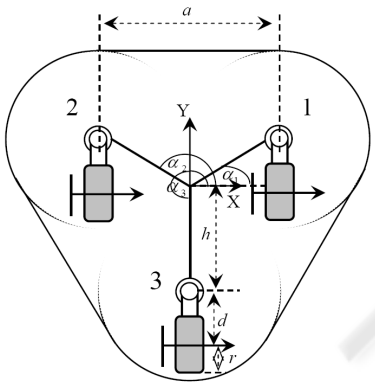

Figure 1: C3P platform configuration.

where

X, Y, ϕ : WMR translation and rotation displacement.

θ_{s_i} : the steering angle for wheel i.

r, d : the wheel radius and the caster wheel offset.

The conventional Caster wheel has three DOF due to the wheel angular velocity $\dot{\theta}_{x_i}$, the contact point angular velocity $\dot{\theta}_{c_i}$ and the steering angular velocity $\dot{\theta}_{s_i}$. The unique thing about the C3P is that it has wheels angular velocities actuation only ($\dot{\theta}_{x_i}$) with no steering angular actuation, which makes the model modular and more challenging.

3 KINEMATICS MODELING AND ANALYSIS

For WMRs' mobility analysis and control, the kinematics modeling is needed. Furthermore, calculating the velocity and acceleration variables are important in the dynamics modeling procedures. In order to analyze and derive the C3P mathematical models, some variables are assigned, such as the following: the robot position vector $p = [X\ Y\ \phi\ ]^T$, the wheel angles vector $q_x = [\theta_{x_1}\ \theta_{x_2}\ \theta_{x_3}]^T$, the steering angles vector $q_s = [\theta_{s_1}\ \theta_{s_2}\ \theta_{s_3}]^T$, and the contact angles vector $q_c = [\theta_{c_1}\ \theta_{c_2}\ \theta_{c_3}]^T$. By differentiating the robot and wheel vectors with respect to time, the robot and wheel velocities are

$$\dot{p} = \frac{dp}{dt},\ \dot{q}_x = \frac{dq_x}{dt},\ \dot{q}_s = \frac{dq_s}{dt},\ \dot{q}_c = \frac{dq_c}{dt}. \quad (1)$$

From the generalized inverse kinematic solution described in (Muir, 1987), the wheel angular velocity inverse kinematic solution is

$$\dot{q_x} = J_{in_x}\dot{p}$$

$$J_{in_x} = \frac{1}{r}\begin{bmatrix} -S(\theta_{s_1}) & C(\theta_{s_1}) & h\,C(\alpha_1 - \theta_{s_1}) \\ -S(\theta_{s_2}) & C(\theta_{s_2}) & h\,C(\alpha_2 - \theta_{s_2}) \\ -S(\theta_{s_3}) & C(\theta_{s_3}) & h\,C(\alpha_3 - \theta_{s_3}) \end{bmatrix} \quad (2)$$

while the steering angular actuation is

$$\dot{q_s} = J_{in_s}\dot{p}$$

$$J_{in_s} = \frac{-1}{d}\begin{bmatrix} C(\theta_{s_1}) & S(\theta_{s_1}) & -h\,S(\alpha_1 - \theta_{s_1}) + d \\ C(\theta_{s_2}) & S(\theta_{s_2}) & -h\,S(\alpha_2 - \theta_{s_2}) + d \\ C(\theta_{s_3}) & S(\theta_{s_3}) & -h\,S(\alpha_3 - \theta_{s_3}) + d \end{bmatrix} \quad (3)$$

and the contact angular velocity inverse solution is

$$\dot{q_c} = J_{in_c}\dot{p}$$

$$J_{in_c} = \frac{-1}{d}\begin{bmatrix} -S(\theta_{s_1}) & C(\theta_{s_1}) & -h\,C(\alpha_1 - \theta_{s_1}) \\ -S(\theta_{s_2}) & C(\theta_{s_2}) & -h\,C(\alpha_2 - \theta_{s_2}) \\ -S(\theta_{s_3}) & C(\theta_{s_3}) & -h\,C(\alpha_3 - \theta_{s_3}) \end{bmatrix} \quad (4)$$

where "C" stands for "cos" and "S" stands for "sin". The solution (2) shows singularities for some steering angles configurations. The singularity appears only when the steering angles are equal. For example, when the steering angles are -90^o, the robot velocity $\dot{Y}$ is not actuated (Fig. (2-a)), and when they are 0^o the velocity $\dot{X}$ is not actuated (Fig. (2-c)). The steering configuration in Fig. (2-b) gives singular determent for the matrix J_{in_x} with -45^o steering angles although all the robot DOFs are actuated.

Obviously, the direction of $[-1\ 1\ 0]^T$ is not actuated, which concludes the following; if all steering angles yield the same value, then the robot is not actuated in the direction parallel to the wheel axes. Fig. (2-d) represents a non-singular steering wheels configuration condition.

Solutions (3) and (4) can be used to overcome the singularity practically by adding practical actuation

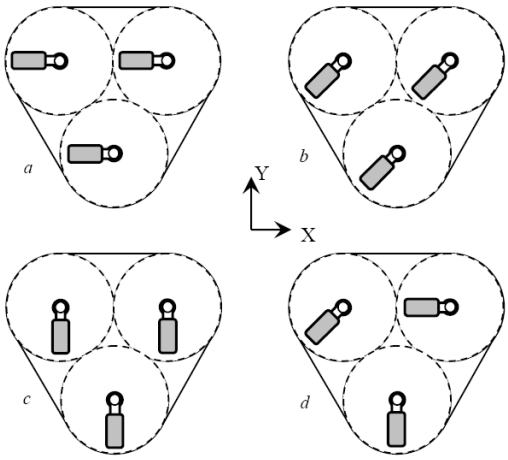

Figure 2: Different steering angles configurations.

to the steering angular velocities, or theoretically by virtually actuating the steering angular velocities (El-Shenawy et al., 2006c).

The forward sensed kinematics used in (El-Shenawy et al., 2006a) shows that the sensed variables are sufficient for robust sensing and slippage detection through the following equation

$$\dot{p} = J_{f_x}\dot{q}_x + J_{f_s}\dot{q}_s, \tag{5}$$

where J_{f_x} and J_{f_s} are the sensed forward solutions for the wheel angular and steering angular velocities respectively. The derivative of equation (5), yields the robot accelerations,

$$\ddot{p} = J_{f_x}\ddot{q}_x + J_{f_s}\ddot{q}_s + g(q_s, \dot{q}_x, \dot{q}_s), \tag{6}$$

from equations (2), (3) and the inversion method proposed in (Muir, 1987) the inverse actuated kinematic accelerations is

$$\begin{bmatrix} \ddot{q}_x \\ \ddot{q}_s \end{bmatrix} = \begin{bmatrix} J_{in_x} \\ J_{in_s} \end{bmatrix} \ddot{p} - g_{cs}(q_s, \dot{p}) \tag{7}$$

4 DYNAMIC MODELING AND ANALYSIS

4.1 Euler Lagrange

The dynamic equations of motion are derived using the Euler-Lagrangian method (Naudet and Lefeber, 2005) based on the Lagrangian function

$$L = K - P, \tag{8}$$

where K denotes the kinetic energy and P denotes the potential energy. Since the C3P is assumed to drive on a planar surface, P is zero.

The Lagrangian dynamic formulation is described as

$$\tau = \frac{d}{dt}\left(\frac{\partial L}{\partial \dot{q}}\right) - \frac{\partial L}{\partial q}, \tag{9}$$

where τ is the vector of actuated torques.

The C3P is considered as a closed chain multi-body system. To derive the dynamic model of the C3P, the system is converted into an open chain structure. First, the dynamic model of each serial chain is evaluated using the Lagrangian dynamic formulation (9). Second, the platform constraints incorporate the open chain dynamics into a closed chain dynamics. The robot consists of 7 parts; 3 identical wheels, 3 identical links and one platform (Fig.(3)).

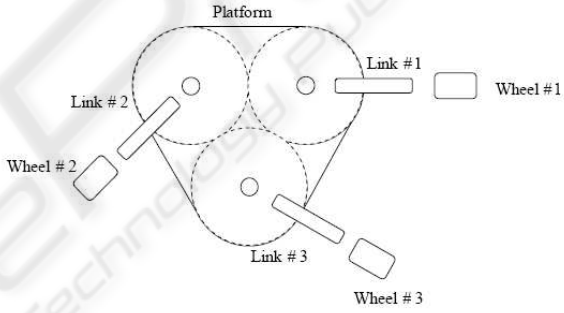

Figure 3: The C3P parts structure.

The kinetic energy of the rigid body depends on its mass, inertia , linear and angular velocities as described by the following equation

$$K = \frac{1}{2}\, m\, V^T\, V + \frac{1}{2}\, \Omega^T\, I\, \Omega \tag{10}$$

where,

m, I : mass and inertia of the rigid body.

V, Ω : linear and angular velocity at the center of gravity of the rigid body.

The sum of the platform kinetic energies equations results in the following Lagrangian function

$$L = \sum_{i=1}^{3} K_{wi} + \sum_{i=1}^{3} K_{li} + K_{pl}, \tag{11}$$

where K_{wi}, K_{li} are the wheel and link i kinetic energies respectively, while K_{pl} is the platform kinetic energy. The wheel co-ordinates q can be considered as the actuated displacements and $\dot{q}$ as the actuated velocities,

while τ is the external torque/force vector. The overall dynamics of the robot can be formulated as a system of ordinary differential equations whose solutions are required to satisfy the WMR constraints through the following force/torques vector equation

$$\tau = M(q)\ddot{q} + G(q,\dot{q}) \quad (12)$$

where, $M(q)$ is the inertia matrix, $G(q,\dot{q})$ contains the centripetal and Coriolis terms.

4.2 Control Structure Design

The C3P control structure contains three main models (Fig.(4)): the forward kinematics for calculating the C3P velocities, the C3P forward dynamic model which models the C3P practical prototype on the simulation level, and the inverse dynamics solution.

The velocity controller (V.C) calculates a control signal u from the velocity error $\dot{e} = \dot{p}_r - \dot{p}_o$, which is added to the reference acceleration signal $\ddot{p}_r$. The reference robot velocities $\dot{p}_r$ and accelerations $\ddot{p}_r$ are used in the inverse dynamic solution to deliver the actuated wheels torques τ_{xa}.

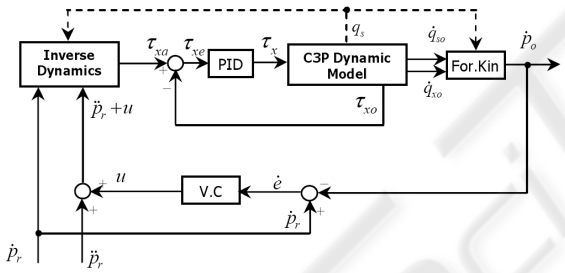

Figure 4: Robot closed-loop structure.

The forward dynamics consists of two main equations; the Wheels Torques Dynamics (WTD) and the Dynamic Steering Estimator (DSE), which were proposed in (El-Shenawy et al., 2006b). The wheel angular velocities are calculated using the wheels torques dynamic equation of motion

$$\tau_x = M(q_s)\ddot{q}_x + G_x(q_s,\dot{q}_x), \quad (13)$$

with respect to the actuated wheels torques, where $\tau_x = [\tau_{x_1}\ \tau_{x_2}\ \tau_{x_3}]^T$. The steering angles and the steering angular wheel velocities are recursively calculated by the steering dynamic estimator

$$\ddot{q}_s = M_{ss}^{-1} M_{xx}\ddot{q}_x + M_{ss}^{-1} G_{ssx}(q_s,\dot{q}_s,\dot{q}_x) \quad (14)$$

corresponding to the angular wheels velocities and accelerations generated due to the applied wheel torque resulting from equation (13).

The C3P dynamic model shown in Fig. (5) has the actuated wheel torques τ_x as an input, while the outputs are the sensed wheel velocities $\dot{q}_x$, the steering angular velocities $\dot{q}_s$, and the steering angles q_s. Since the steering angular velocities are actuated by the angular wheel velocities, the angular wheel velocities $\dot{q}_x$ and accelerations $\ddot{q}_x$ are the main inputs of the steering dynamic estimator. The steering angles q_s and steering angular velocities $\dot{q}_s$ are delayed by unity time interval because the steering dynamic model is calculated recursively according to (14).

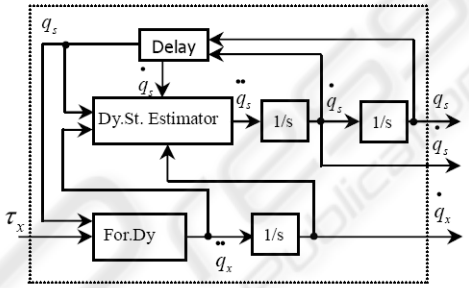

Figure 5: The C3P Dynamic Model.

The inverse dynamic solution proposed is implemented in the velocity control loop to overcome the singularity with simpler velocity controller and better performance. The inverse dynamic equation depends on the platform constraints, which are described in the forward kinematic solution. They are combined using Lagrangian formulation and the dynamic torque equation (9) to obtain the described wheel torques equation

$$\tau_{x_a} = \begin{bmatrix} M_{x_a} & M_{s_a} \end{bmatrix} \begin{bmatrix} \ddot{q}_x \\ \ddot{q}_s \end{bmatrix} + G_{sx_a}(\dot{q}_x,\dot{q}_s,q_s) \quad (15)$$

The matrix M_{x_a} is the inverse dynamic solution for actuating the wheels torques τ_{x_a}, while the matrix M_{s_a} is the inverse dynamic solution for actuating the steering angular acceleration $\ddot{q}_s$ using the wheel torques τ_{x_a}. The inverse dynamics solution is a relation between the desired robot velocities and accelerations ($\dot{q}$, $\ddot{q}$) as an input and the actuated applied torques of the wheels (τ_{x_a}) as an output. However, the dynamic torque equation (15) is a function of $\ddot{q}_x$, $\ddot{q}_s$, $\dot{q}_x$, and $\dot{q}_s$. By using the velocity and acceleration inverse kinematic solutions(2, 3, 4 and 7), the desired torque equation is achieved and the actuation characteristics of the steering angular velocities and accelerations are included in the inverse dynamic solution as well. As a result the actuated torques equation will have the robot velocities $\dot{p}$ and accelerations $\ddot{p}$ as input variables

$$\tau_{x_a} = M_x(q_s)\ddot{p} + G_{xi}(q_s,\dot{p}) \quad (16)$$

$$M_x = \begin{bmatrix} M_{x_a} & M_{s_a} \end{bmatrix} \begin{bmatrix} J_{in_x} \\ J_{in_s} \end{bmatrix}, \quad (17)$$

$$G_{xi} = G_{sx_a}(q_s, \dot{p}) - \begin{bmatrix} M_{x_a} & M_{s_a} \end{bmatrix} g_{cs}(q_s, \dot{p}) \quad (18)$$

4.3 Model Analysis

The proposed inverse and forward dynamic solutions are different in structure and mathematical representation as well. However, both models should yield the inversion of each other. Therefore some simulation examples are done and analyzed in this section to illustrate the performance of the model. The simulations are done using the structure shown in Fig. (4) with zero values for the velocity (V.C.) and the axes level control parameters to disable their effects. The C3P parameters are set to be exactly like the practical prototype, which are described in Table 1.

Table 1: The C3P parameters.

C3P Parameters	Value	Units
h	0.343	m
d	0.04	m
r	0.04	m
M_p (Platform mass)	25	Kg
I_p (Platform inertia)	3.51	$Kg\ m^2$

Fig.(6) shows a comparison between two different examples. The first example is a non singular condition, where the steering angles are $\theta_{s_1} = \theta_{s_2} = \theta_{s_3} = 0^o$ as shown in Fig. (2c). The input signal is a ramp input in Y direction while the X translational and Φ velocities are zeros. The input V_y or $\dot{Y}$ is a ramp signal till 3.2 seconds then it is constant. The second example is a non singular condition but with different steering angles, where $\theta_{s_1} = 45^o$,$\theta_{s_2} = -45^o$ and $\theta_{s_3} = 90^o$ with the same ramp input signal. Fig. (6-a) shows the trajectory of the steering angles, which are indicated as (θ_{s-oi}) for example one and (θ_{s-i}) for example two.

The reference input velocities maintain zero steering angles value. For the first example, the steering angles keep their initial value, while in the second example the steering angles were adjusted from their initial value to the zero value. The steering wheel adjustment took place due to the the step acceleration input in Y direction. The robot output velocity and acceleration $Out-1$ result from the first example (Fig. (6-b) &(6-c)), which follow the input signal as well as the steering and wheel angular accelerations (α_{s-oi},α_{x-oi}) as shown in Fig. (6-d) &(6-e).

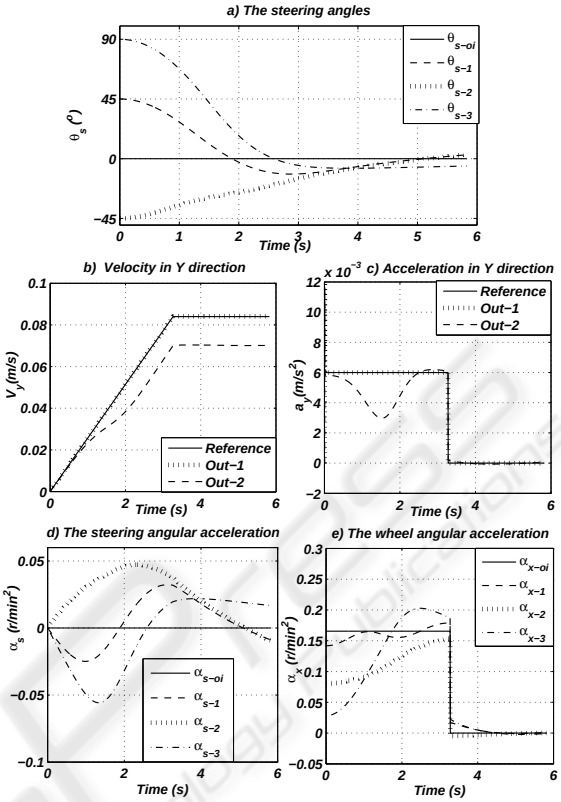

Figure 6: Simulation comparison for ramp input.

For the second example, the input acceleration and the initial steering angles produce disturbances and oscillations in the wheel angular acceleration (($\alpha_{x_i} = 0$ for i $\in$ {1,2,3} (Fig. (6-e)))). Such disturbances produce oscillations in the steering angular accelerations (($\alpha_{s_i} = 0$ for i $\in$ {1,2,3} (Fig. (6-d)))), which results negative overshoot in the robot Y acceleration ($Out-2$) (Fig. (6-c))). In addition to the presence of the dynamic delay in the forward dynamics solution (Fig. (5)) and some simulation numerical errors the overshoot appears.

When the robot velocity takes constant value the desired wheel acceleration suddenly change from value 0.17 (r/min^2) to 0 (r/min^2). Such input does not cause multiple oscillations or high overshoots in output signal (Fig. (6-d)).

The next simulation shows the responses of the robot velocities and accelerations after enabling the axes and robot level controllers. The robot starts from the same initial steering angles but the input velocity is ramp signal in X direction and Zero value in the Y and the rotational velocities (Fig.(7-d)). Such input yields the steering angles to reach -90^o (Fig.(7-a)), which is adjusted due to the wheel angular accelera-

tions oscillations resulted in Fig. (7-b).

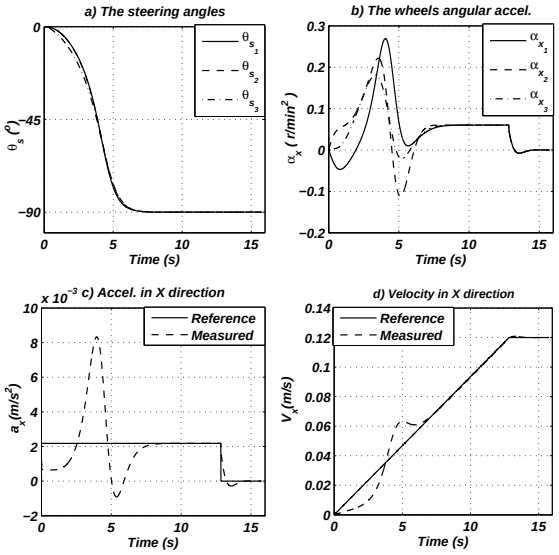

Figure 7: simulation responses for ramp input with singularity configuration.

In the first seven seconds during the steering angles adjustment, the output acceleration of the robot X direction oscillates but it reach the desired value as the steering angles settle with their desired values (Fig.(7-c)). These oscillations affect the robot velocity output as well by oscillating around the desired signal (Fig.(7-d)). In case of having Y as adesired direction, the output signal will be exactly the same like the input, because the effect of the delay unit in the forward dynamics solution is negligible.

5 LAB EXPERIMENT

After analyzing the inverse and forward dynamic solutions, the inverse dynamic solution is implemented on the C3P prototype (Fig. (8)) to test its performance practically. Therefore, an experiment was implemented in the lab with the following initial steering angles $\theta_{s_1} = \theta_{s_2} = \theta_{s_3} = 135^o$ and input robot velocities $\dot{p}_r = [0.5(m/s)\ \ 0.5(m/s)\ \ 0(r/min)]^T$. Such input velocities yields the steering angles to flip 180^o to reach -45^o or 315^o values (Fig.(9-a)).

The steering angles θ_{s_2} and θ_{s_3} flipped after 2 seconds in different directions (Fig.9c), causing oscillations in the robot velocities (Fig.(9-d), (9-e) & (9-f)). After the fourth second, the first steering angle θ_{s_1} flipped producing another overshoots in the robot velocities. The robot velocities (Fig.(9-d), (9-e) & (9-f))

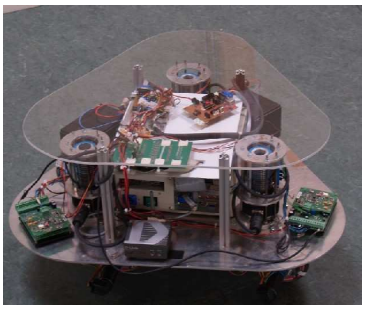

Figure 8: The C3P practical prototype.

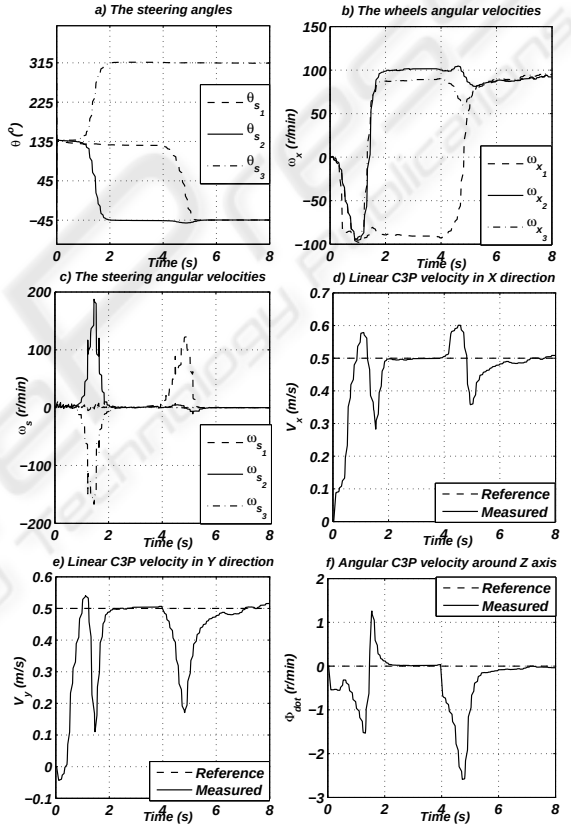

Figure 9: Practical Lab results for the C3P prototype.

are measured with respect to the floor frame of coordinates, which illustrates how the responses follow the reference value in the steady state.

The main advantage and main problem of the C3P configuration are the same. This is the non direct actuation of the steering angular velocities of the wheel. Such a problem is very challenging from the theoretical and practical point of view. Since the steering angular velocities are virtually actuated, their behavior can not be exactly predicted. However, the for-

ward dynamic model is the main factor in deriving the inverse dynamic solution and designing its control structure along with tuning its parameters. These information are very useful during the practical implementation takes place, as in the last experiment.

6 CONCLUSION

The kinematics and the dynamics models of the holonomic mobile robot C3P are presented in this paper. The singularity problem found in such actuation configuration is described by the inverse kinematic solution. The dynamic analysis showed the effect of the wheel and steering angular accelerations of the caster wheels on the inverse dynamic behavior with and without velocity controllers. Although the inverse and forward dynamic models are different in structure, they yield the inversion of each other. The steering angular acceleration plays a very important rule in calculating the reference actuated signal to the platform to overcome the robot singularities and to adjust its steering angles. The simulation examples showed the model dynamic analysis through the robot acceleration variables, and the practical experiment proved the effectiveness of the control structure.

REFERENCES

Albagul, A. and Wahyudi (2004). Dynamic modelling and adaptive traction control for mobile robots. *Int. Jor. of Advanced Robotic Systems, Vol.1,No.3*.

Asensio, J. R. and Montano, L. (2002). A kinematic and dynamic model-based motion controller for mobile robots. *15th Triennial World Congress*.

Bruemmer, J., Marble, J., and Dudenhoffer, D. (1998). Intelligent robots for use in hazardous dor environments.

Burgard, W., Trahanias, P., Haehnel, D., Moors, M., Schulz, D., Baltzakis, H., and Argyros, A. (2002). Tourbot and webfair: Web-operated mobile robots for telepresence in populated exhibitions. *IEEE/RSJ Conf. IROS'02, Full day workshop in "Robots in Exhibitions*.

Chakravarty, P., Rawlinson, D., and Jarvis, R. (2004). Distributed visual servoing of a mobile robot for surveillance applications. *Australasian Conference on Robotics and Automation (ACRA)*.

El-Shenawy, A., Wagner, A., and Badreddin, E. (2006a). Controlling a holonomic mobile robot with kinematics singularities. *The 6th World Congress on Intelligent Control and Automation*.

El-Shenawy, A., Wagner, A., and Badreddin, E. (2006b). Dynamic model of a holonomic mobile robot with actuated caster wheels. *The 9th International Conference on Control, Automation, Robotics and Vision, ICARCV*.

El-Shenawy, A., Wagner, A., and Badreddin, E. (2006c). Solving the singularity problem for a holonomic mobile. *4th IFAC-Symposium on Mechatronic Systems (MECHATRONICS 2006)*.

Fulmer, C. R. (2003). Design and fabrication of an omnidirectional vehicle platform. *Master thesis University of Florida*.

Kartoun, U., Stern, H., Edan, Y., Feied, C., Handler, J., Smith, M., and Gillam, M. (2006). Vision-based autonomous robot self-docking and recharging. *11th International Symposium on Robotics and Applications (ISORA)*.

Khatib, O., Jaouni, H., Chatila, R., and Laumond, J. P. (1997). Dynamic path modification for car-like nonholonomic mobile robots. *IEEE Intl. Conf. on Robotics and Automation*.

Moore, K. and Flann, N. (2000). Six-wheeled omnidirectional autonomous mobile robot. *IEEE Control Systems Magazine*.

Muir, P. (1987). Modeling and control of wheeled mobile robots. *PhD dissertation Carnegie mellon university*.

Naudet, J. and Lefeber, D. (2005). Recursive algorithm based on canonical momenta for forward dynamics of multibody systems. *Proceedings of IDETC/CIE*.

Peng, Y. and Badreddin, E. (2000). Analyses and simulation of the kinematics of a wheeled mobile robot platform with three castor wheels.

Ramírez, G. and Zeghloul, S. (2000). A new local path planner for nonholonmic mobile robot navigation in cluttered environments. *IEEE Int. Conf. on Robotics and Automation*.

Steinbauer, G. and Wotawa, F. (2004). Mobile robots in exhibitions, games and education. do they really help? *CLAWAR/EURON Workshop on Robots in Entertainment, Leisure and Hobby*.

Yamashita, A., Asama, H., Kaetsu, H., Endo, I., and Arai, T. (2001). Development of omni-directional and step-climbing mobile robot. *Proceedings of the 3rd International Conference on Field and Service Robotics (FSR2001)*.

Yun, X. and Sarkar, N. (1998). Unified formulation of robotic systems with holonomic and nonholonomic constrains. *IEEE Trans. on robotics and automation, Vol.12, pp.640-650*.